A Tunable Broadband Terahertz Absorber Based on Graphene Frequency Selective Surfaces

Elahe Torabi
Department of Electrical and
Computer Engineering
Shiraz University
Shiraz, Iran
Email: elahetorabi20@gmail.com

Alireza Yahaghi
Department of Electrical and
Computer Engineering
Shiraz University
Shiraz, Iran

***Abstract*—A broadband THz absorber is presented which is based on frequency selective surfaces (FSS). In order to make the design tunable, graphene is used in the patch layer. Random hill climbing algorithm has been applied to find the optimum design corresponding to the broadest bandwidth. A 43% bandwidth at low terahertzs is obtained by the optimum design.**

I. Introduction

Frequency band between 100 GHz and 30 THz is typically regarded as the terahertz band [1]. Technology related to this territory is young but it is growing fast in diverse fields such as communication and sensing [1]. To actualize potential applications, developing devices capable of operating at the THz frequencies is necessary. THz absorbers are one of the devices usually needed for setting up many THz experiments.

An absorber absorbs an incident electromagnetic wave which is realized by considerably low reflection or transmission of the wave depending on the application [2], [3]. For example a radar absorber reduces the radar cross section (RCS) by minimizing the reflectance of incident waves from the object [3]. Recently, THz absorbers which are specially developed to manipulate THz waves have attracted many research interests and found applications in areas such as imaging [4], sensing [5] and stealth technology [6].

Different types of THz absorbers have been demonstrated. Salisbury [7], pyramidal [8] and FSS absorbers [9]–[12] are some to name, each of which has special mechanism for absorption. A FSS absorber consists of a grounded substrate which is covered by a periodic patch layer on top [3]. This structure resonates at some frequencies. Consequently the energy is captured and then dissipated by lossy parts of the structure [3]. In this situation, absorption is obtained by (1) [9], [10].

$$A = 1 - |S_{11}|^2 \tag{1}$$

To make FSSs tunable, different techniques have been introduced. Varactor diodes [13], liquid crystals [14] or microelectromechanical systems (MEMS) switches [15] are the frequent ones. However these methods face limitations at THz frequencies [16]. Graphene can be a potential candidate to overcome these limitations in accordance with integration, miniaturization, biasing complexity and operational frequency [16]. Graphene is a one-atom thick carbon layer which consists of carbon atoms arranged in a chicken-wire-like structure [17]. Discovered in 2004 [18], this material has a tunable conductance which can be changed by electrostatic or magnetostatic field or by chemical modification [19].

There are several reports on tunable THz absorbers which are graphene based periodic structures [9]–[12]. For instance, narrowband and broadband THz absorbers with continuous graphene patch and structured substrate have been reported [10]. In [11], a unit cell which is a combination of cross-shaped gold resonator and double layer graphene wires to demonstrate a polarization independent absorber has been suggested . Here, the shape and material of the patches are decided by an optimization algorithm which is explained in the following section.

II. Design

The frequency range considered here is 0.1 to 4 terahertz (low terahertzs). To design the FSS absorber, one needs to determine the characteristics of the substrate, the patch and the periodicity of the array [20]. Except the patch layer, other parameters are decided and fixed during optimization. The height of the substrate (h) and the periodicity of the array in both x (P_x) and y (P_y) directions are set to 20 and 80 micrometers respectively (Fig. 1). A lossy polymer with relative permittivity, $\varepsilon_r = 3.5 + 0.2j$ [11] is assigned to the substrate. The optimization algorithm determines the shape and material of the patches. Being the optimum algorithm for optimization of FSS structures [20], randomly initialized hill climbing algorithm (RHC) is applied to find the optimum patch layer. Graphene is one of the materials chosen for the patch construction in order to make the absorber tunable. To analyze designs with graphene, an electromagnetic model of graphene is necessary and it is demonstrated in section A. Section B describes the optimization process. Normal incidence is considered during all electromagnetic analyses.

A. Graphene Model

Graphene is modeled by a surface conductivity. Without a magnetostatic bias field or spatial dispersion, graphene conductivity is introduced by (2) [19]. To tune the surface

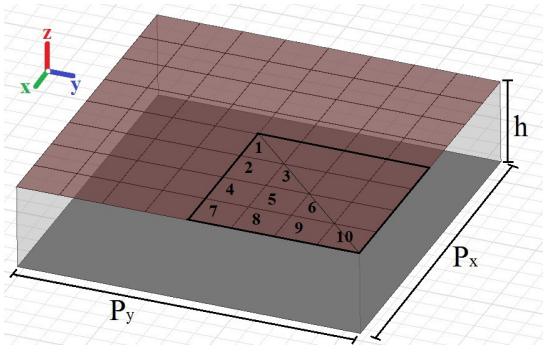

Fig. 1: Unit cell of the FSS absorber

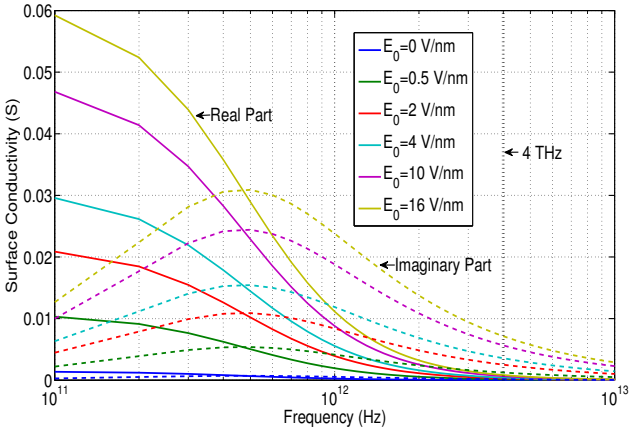

Fig. 2: Surface conductivity of the graphene

conductivity, an electrostatic bias field is applied and the spatial dispersion is negligible here [21].

$$\sigma(\omega,\mu(\mathbf{E_0}),\Gamma,T) = \frac{je^2(\omega-j2\Gamma)}{\pi\hbar^2}\{\frac{1}{(\omega-j2\Gamma)^2}\int_0^\infty \varepsilon\left(\frac{\partial f_d(\varepsilon)}{\partial\varepsilon}-\frac{\partial f_d(-\varepsilon)}{\partial\varepsilon}\right)d\varepsilon - \int_0^\infty \frac{f_d(-\varepsilon)-f_d(\varepsilon)}{(\omega-j2\Gamma)^2-4\left(\frac{\varepsilon}{\hbar}\right)^2}d\varepsilon\} \quad (2)$$

$$f_d(\varepsilon) = \frac{1}{1+e^{(\varepsilon-|\mu_c|)/k_BT}} \quad (3)$$

Where ω is the frequency in radian, Γ is a phenomenological electron scattering rate which is assumed to be independent of energy ε, T is the temperature, $-e$ is an electron charge, $\hbar = h/2\pi$ is the reduced Plank's constant, $f_d(\varepsilon)$ is the Fermi-Dirac distribution (3), k_B is the Boltzmann's constant and μ_c is the chemical potential which is dependent on electrostatic bias field ($\mathbf{E_0}$) [19]. The phenomenological scattering rate is $(1/2\tau)$ [22]. τ is the phenomenological scattering time which is set to 0.34 picoseconds [23], [24]. T is considered to be equal to the room temperature (300 K). The surface conductivity versus frequency for different values of electrostatic bias is shown in Fig. 2. To model graphene in HFSS, surface impedance ($Z_s = 1/\sigma$) is assigned to the graphene sheet as a boundary condition [16], [22]. The surface impedance versus frequency for different values of electrostatic bias is shown in Fig. 3. It evidences that the more bias voltage is, the more conductive the graphene sheet will be.

B. Optimization

The RHC algorithm generates bit strings each of which is a code for a design. The surface of the unit cell is divided into $N \times N$ pixels (Fig. 1). The codes determine the material assigned to each of these pixels. To increase the degrees of freedom, four options are provided for a single pixel, gold, graphene with $\mu_c = 0.775$ eV ($E_0 = 4V/nm$) which will be biased, graphene with the same chemical potential which is fixed by chemical doping modification, and air. Two bits are adopted to represent these materials. $\{00\}$, $\{11\}$, $\{10\}$ and $\{01\}$ represent gold, biased graphene, unbiased graphene and air respectively.

Symmetries with respect to x and y directions as well as the bisectors are applied (Fig. 1). This makes the electromagnetic response independent of polarization under normal incidence [9]. Besides, one eighth of the shape dictates the whole configuration which causes a drastic reduction in the number of possible designs. In this paper, N is set to 8. Therefore a string of 20 bits is enough to code the whole shape of the patch.

Pixels to which biased graphene is assigned need to be connected in order to apply bias voltage only at one single location. These pixels can be also connected through gold ones. This way, we end up with a bias chain which consists of biased graphene and gold pixels and must be isolated from unbiased graphene ones.

When RHC algorithm generates each 20-bit-string, two MATLAB functions are called. The first one evaluates whether the bit string is an acceptable one regarding to the bias conditions or not and outputs 1 or 0 respectively. If the output is 0, the string will be discarded, else the second function called fitness function gets the bit string as an input. Fitness function provides a VBScript of the whole design according to the bit string and earlier assumptions. The function runs the script using commercial software HFSS 13.0 and calculates the scattering parameter, S_{11} at each frequency step. Fitness function determines the absorption (1) and then the bandwidth and passes it to the optimization algorithm. To check the bandwidth of the designs, least absorption of 80% is considered. The optimization algorithm saves the string with the returned bandwidth in a table. After reaching a specific number of fitness evaluation, the design with maximum bandwidth will be announced.

III. RESULTS

An optimization with maximum number of evaluation equal to 1000, and 10 random initial values has been run.

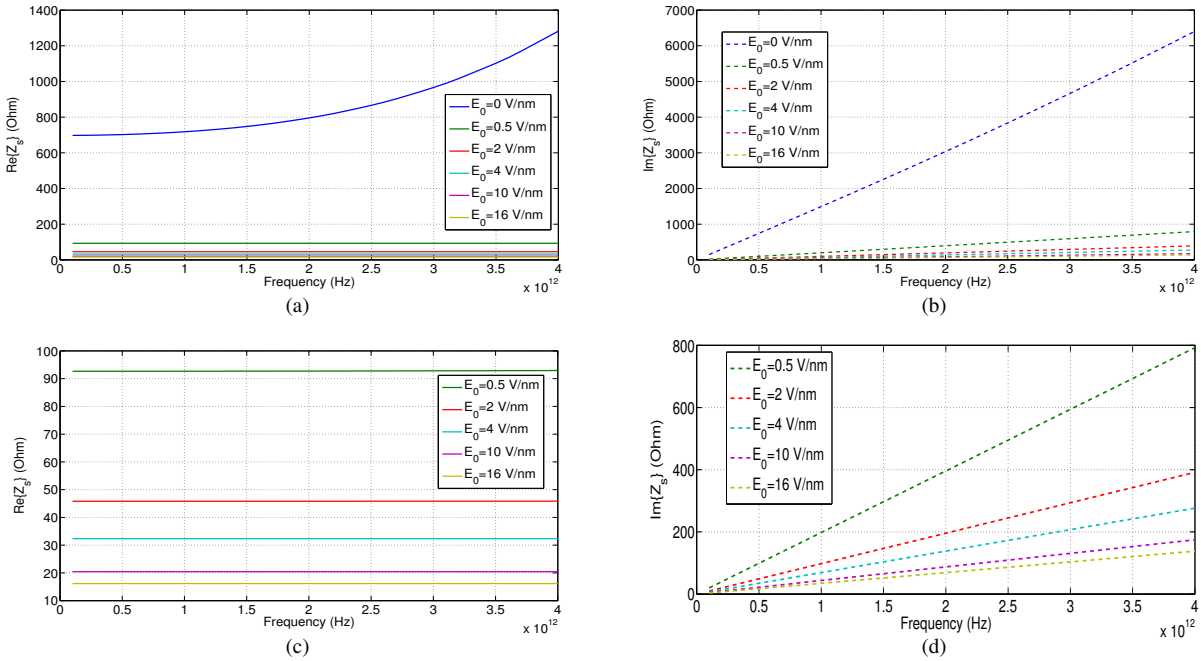

Fig. 3: (a) Real and (b) Imaginary part of the surface impedance for biased and unbiased graphene (c) Real and (d) Imaginary part of the surface impedance for biased graphene

103rd {0101011010010001011O} and 551st evaluated designs {0101011111010001011O} have the broadest bandwidth of about 1.68 THz (Fig. 4). Reinitialization during the optimization is equal to 8132 which exceeds 1000 maximum evaluations becuase the wrong designs in accordance with bias chain were discarded. According to the convergence diagram (Fig. 5), the optimization converged after about 100 fitness evaluations. This fact accompanied with the large amount of reinitialization almost assures that the best patch design is achieved.

Both optimum designs are actually the same and thus have the same absorption if the same chemical potential of 0.775 eV is assigned to both graphene types. That's why only the schematic of the 551st design is depicted in Fig. 4 in which gray pixels are biased graphene, brown ones are unbiased graphene and yellow ones are gold. However the 551st design has biased graphene which makes tuning possible. The frequency response of this design under different bias voltages is shown by Fig. 6. As it is noticed from the figure, different absorption levels are achivable.

The absorption of the same structure with a layer of graphene as the whole patch is also examined by different bias voltages. Fig. 7 proves that, although tuning is well done by such design, the broadest bandwidth is still narrow (almost 0.2 THz). Therefore patterning and optimization have improved the bandwidth pronouncedly.

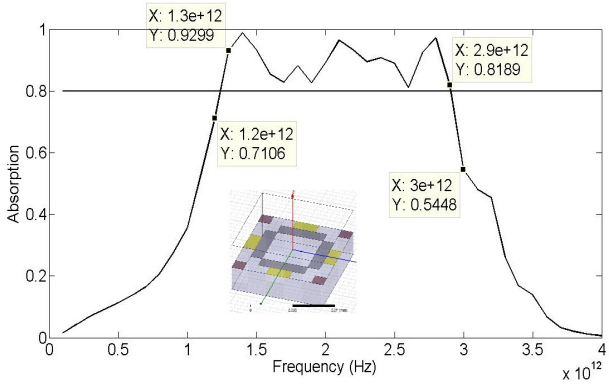

Fig. 4: Absorption for the optimum design of the patch layer

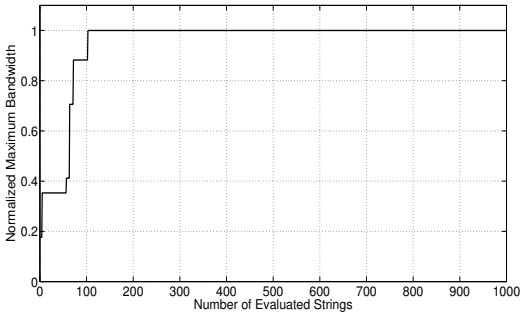

Fig. 5: Convergence

IV. Conclusion

A FSS absorber has been presented which is designed for low terahertzs. Graphene is used as a material in the patch layer which provides a simple tuning mechanism. Using random hill climbing algorithm, an optimized design with 43% bandwidth of about 1.68 THz is achieved.

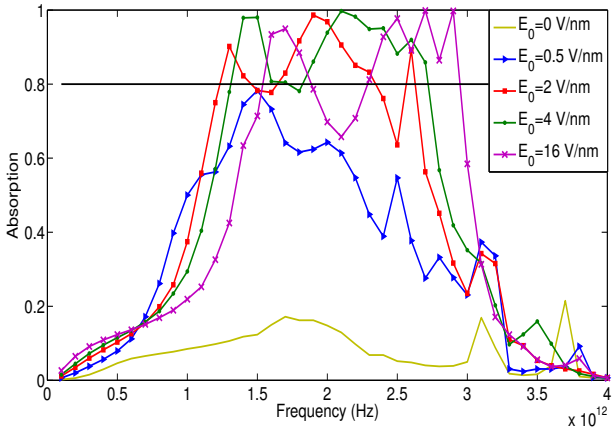

Fig. 6: Tuning the frequency response of the optimum design by various bias voltages

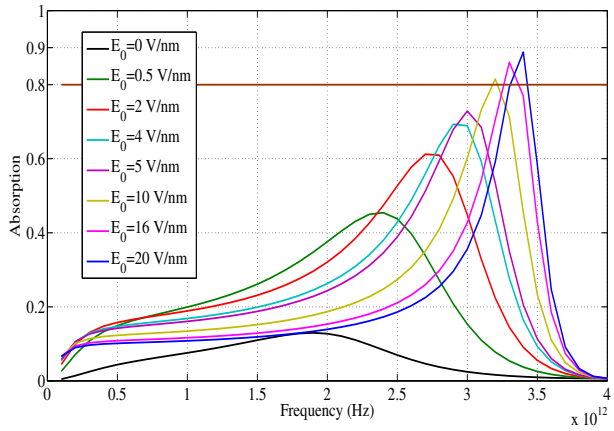

Fig. 7: Absorption of the structure with a layer of graphene as a patch layer for different bias voltages

REFERENCES

[1] M. Tonouchi, "Cutting-edge terahertz technology," *Nature photonics*, vol. 1, no. 2, pp. 97–105, 2007.

[2] C. M. Watts, X. Liu, and W. J. Padilla, "Metamaterial electromagnetic wave absorbers," *Advanced materials*, vol. 24, no. 23, pp. OP98–OP120, 2012.

[3] A. Fallahi, A. Yahaghi, H.-R. Benedickter, H. Abiri, M. Shahabadi, and C. Hafner, "Thin wideband radar absorbers," *Antennas and Propagation, IEEE Transactions on*, vol. 58, no. 12, pp. 4051–4058, 2010.

[4] S. A. Kuznetsov, A. G. Paulish, A. V. Gelfand, P. A. Lazorskiy, and V. N. Fedorinin, "Matrix structure of metamaterial absorbers for multispectral terahertz imaging," *Progress In Electromagnetics Research*, vol. 122, pp. 93–103, 2012.

[5] N. Liu, M. Mesch, T. Weiss, M. Hentschel, and H. Giessen, "Infrared perfect absorber and its application as plasmonic sensor," *Nano letters*, vol. 10, no. 7, pp. 2342–2348, 2010.

[6] K. Iwaszczuk, A. C. Strikwerda, K. Fan, X. Zhang, R. D. Averitt, and P. U. Jepsen, "Flexible metamaterial absorbers for stealth applications at terahertz frequencies," *Optics express*, vol. 20, no. 1, pp. 635–643, 2012.

[7] J. M. Woo, M.-S. Kim, H. W. Kim, and J.-H. Jang, "Graphene based salisbury screen for terahertz absorber," *Applied Physics Letters*, vol. 104, no. 8, p. 081106, 2014.

[8] S. He and T. Chen, "Broadband thz absorbers with graphene-based anisotropic metamaterial films," *Terahertz Science and Technology, IEEE Transactions on*, vol. 3, no. 6, pp. 757–763, 2013.

[9] A. Andryieuski and A. V. Lavrinenko, "Graphene metamaterials based tunable terahertz absorber: effective surface conductivity approach," *Optics express*, vol. 21, no. 7, pp. 9144–9155, 2013.

[10] B.-z. Xu, C.-q. Gu, Z. Li, and Z.-y. Niu, "A novel structure for tunable terahertz absorber based on graphene," *Optics express*, vol. 21, no. 20, pp. 23 803–23 811, 2013.

[11] Y. Zhang, Y. Feng, B. Zhu, J. Zhao, and T. Jiang, "Graphene based tunable metamaterial absorber and polarization modulation in terahertz frequency," *Optics express*, vol. 22, no. 19, pp. 22 743–22 752, 2014.

[12] M. Amin, M. Farhat, and H. Bağcı, "An ultra-broadband multilayered graphene absorber," *Optics express*, vol. 21, no. 24, pp. 29 938–29 948, 2013.

[13] F. Bayatpur and K. Sarabandi, "A tunable metamaterial frequency-selective surface with variable modes of operation," *Microwave Theory and Techniques, IEEE Transactions on*, vol. 57, no. 6, pp. 1433–1438, 2009.

[14] W. Hu, R. Dickie, R. Cahill, H. Gamble, Y. Ismail, V. Fusco, D. Linton, N. Grant, and S. Rea, "Liquid crystal tunable mm wave frequency selective surface," *Microwave and Wireless Components Letters, IEEE*, vol. 17, no. 9, pp. 667–669, 2007.

[15] M. H. Ucar, A. Sondas, and Y. E. Erdemli, "Switchable split-ring frequency selective surfaces," *Progress In Electromagnetics Research B*, vol. 6, pp. 65–79, 2008.

[16] A. Fallahi and J. Perruisseau-Carrier, "Design of tunable biperiodic graphene metasurfaces," *Physical Review B*, vol. 86, no. 19, p. 195408, 2012.

[17] A. K. Geim and K. S. Novoselov, "The rise of graphene," *Nature materials*, vol. 6, no. 3, pp. 183–191, 2007.

[18] K. S. Novoselov, A. K. Geim, S. Morozov, D. Jiang, Y. Zhang, S. Dubonos, , I. Grigorieva, and A. Firsov, "Electric field effect in atomically thin carbon films," *science*, vol. 306, no. 5696, pp. 666–669, 2004.

[19] G. W. Hanson, "Dyadic green's functions for an anisotropic, non-local model of biased graphene," *Antennas and Propagation, IEEE Transactions on*, vol. 56, no. 3, pp. 747–757, 2008.

[20] A. Fallahi, M. Mishrikey, C. Hafner, and R. Vahldieck, "Efficient procedures for the optimization of frequency selective surfaces," *Antennas and Propagation, IEEE Transactions on*, vol. 56, no. 5, pp. 1340–1349, 2008.

[21] J. S. Gomez-Diaz, J. R. Mosig, and J. Perruisseau-Carrier, "Effect of spatial dispersion on surface waves propagating along graphene sheets," *Antennas and Propagation, IEEE Transactions on*, vol. 61, no. 7, pp. 3589–3596, 2013.

[22] J.-S. Gómez-Díaz and J. Perruisseau-Carrier, "Graphene-based plasmonic switches at near infrared frequencies," *Optics express*, vol. 21, no. 13, pp. 15 490–15 504, 2013.

[23] J. Y. Kim, C. Lee, S. Bae, K. S. Kim, B. H. Hong, and E. Choi, "Far-infrared study of substrate-effect on large scale graphene," *Applied Physics Letters*, vol. 98, no. 20, p. 201907, 2011.

[24] C. Lee, J. Y. Kim, S. Bae, K. S. Kim, B. H. Hong, and E. Choi, "Optical response of large scale single layer graphene," *Applied Physics Letters*, vol. 98, no. 7, p. 071905, 2011.